

**UNIVERSITY GRANTS COMMISSION  
BAHADUR SHAH ZAFAR MARG  
NEW DELHI – 110 002**

**PROFORMA FOR SUBMISSION OF INFORMATION AT THE TIME OF SENDING  
THE FINAL REPORT OF THE WORK DONE ON THE PROJECT**

1. TITLE OF THE PROJECT : “Fabrication and characterization of Reduced graphene oxide Field Effect Transistors (rGO -FET) for sensor applications”
2. NAME AND ADDRESS OF THE PRINCIPAL INVESTIGATOR  
Dr. Goverdhan Reddy Turpu  
Department of Pure and Applied Physics  
Guru Ghasidas Viswavidyalaya, Koni, Bilaspur 495009
3. NAME AND ADDRESS OF THE INSTITUTION  
Department of Pure and Applied Physics  
Guru Ghasidas Viswavidyalaya, Koni, Bilaspur 495009
4. UGC APPROVAL LETTER NO. AND DATE 43-407/2014 (SR), 07 Sept. 2015
5. DATE OF IMPLEMENTATION .....01/07/2015
6. TENURE OF THE PROJECT .....03 Years..... ✓
7. TOTAL GRANT ALLOCATED ..... Rs. 10,20,500.00 ✓
8. TOTAL GRANT RECEIVED ..... Rs. 9,23,000=00 ..... ✓
9. FINAL EXPENDITURE ..... Rs. 79,344 =00 ✓
10. TITLE OF THE PROJECT “Fabrication and characterization of Reduced graphene oxide Field Effect Transistors (rGO -FET) for sensor applications”
11. OBJECTIVES OF THE PROJECT
  - Synthesis of graphene oxide (GO) through modified hummer’s method and reduction of GO to reduced graphene oxide (rGO) through chemical methods.
  - Characterization of the GO and rGO through XRD, and Raman spectroscopic studies
  - GO Film fabrication on Si/SiO<sub>2</sub> (300 nm) and patterning of GO film as a micro channel with the combination of photolithography and oxygen plasma etching
  - Characterization of rGO – FETs using I – V characteristics and study adsorbate effects on electrical properties
  - During Mid - term evaluation, the additional work related to photocatalytic and electrochemical applications of the composites of the rGO with functional materials was also discussed and presented
12. WHETHER OBJECTIVES WERE ACHIEVED ..... Yes.....  
(Give Details)
  - Graphene Oxide and reduced Graphene Oxide were synthesized successfully using proposed methods and characterized thoroughly
  - X – ray Diffraction, Transmission Electron Microscopy, Scanning Electron Microscopic studies were done on the samples to confirm their formation

- Raman Spectroscopic studies were done on all the sample to confirm the SP<sup>2</sup> hybridized C- structures in the materials to confirm the Graphene Oxide formation
- Several Composites of the reduced Graphene Oxide (rGO) were synthesized through different chemical methods like co precipitation assisted sonochemical method, solid state synthesis assisted sonochemical methods.
- rGO-SnO<sub>2</sub> compounds were synthesized and studied for photocatalytic applications to degrade the Industrial dye, UJALA Blue , Methylene Orange and Super capacitor applications, there results appeared in *IOP Conf. Series: Materials Science and Engineering* 149 (2016) 012169 and *AIP Conf. Proceedings* 1728 (2016) 020375
- rGO-FeVO<sub>4</sub> compounds were synthesized and studied for photocatalytic and super capacitor applications in both bulk and nano sizes. The results appeared in *Applied Surface Science* 488(2019)221 *AIP Conf Proc.* 2220(2020)080070
- rGO – CrVO<sub>4</sub> compounds were synthesized and studied for photocatalytic and super capacitor behaviour and these results appeared in *J. Phy. Chem. C* 122 (2018)21140
- rGO – V<sub>2</sub>O<sub>5</sub> composite compounds were synthesized and studied for photocatalytic applications and these results appeared in *J. Alloys and Compounds* Article # 155746 ([doi.org/10.1016/j.jallcom.2020.155746](https://doi.org/10.1016/j.jallcom.2020.155746))

### 13. ACHIEVEMENTS FROM THE PROJECT

- ✓ A novel and easy method for the synthesis of rGO – composites was developed and implemented successfully
- ✓ Rapid Photodegradation of Methylene Blue, an industrial dye is being implemented which would be a very interesting results and paves way to develop rapid photocatalytic materials
- ✓ Project produced high quality research publication including journals like JPCC(ACS) (I.F. 4.3), App Surf Sci (I.F. 5.17) and J. Alloys and Comp. (I.F. 4.15)

### 14. SUMMARY OF THE FINDINGS

The project was aimed at development of novel reduced graphene oxide based sensors and multifunctional composite materials. During the duration of the project, reduced graphene oxide was successfully synthesized through modified Hummer's method followed by the reduction using chemical methods. The synthesized rGO was thus used to prepare the composite materials. Several interesting multifunctional materials like FeVO<sub>4</sub>, CrVO<sub>4</sub>, V<sub>2</sub>O<sub>5</sub> and SnO<sub>2</sub> were synthesized through solid state reaction, co-precipitation methods to achieve bulk and nano particles. Composites of these materials were prepared through simple sonochemical mixing method which yielded uniformly mixed composite materials. This was confirmed by SEM and TEM measurements on these materials. Cyclic Voltammetric measurements were done on the samples to study the super capacitor behaviour on these systems these results were supported by DFT calculations through the help of our collaborators at BARC, Mumbai. Photocatalytic degradation of Methylene Blue dye was studied by all the composite materials where we could develop a rapid photocatalyst which degrades MB in 20 minutes with 70% dye removal capacity.

15. CONTRIBUTION TO THE SOCIETY .....

Photocatalytic degradation of industrial affluent is a quite interesting results pertaining to the environmental remediation in the current world. The method developed for the rapid photo degradation of MB will be a huge step forward for us to develop prototype filter membranes for industrial waste water and this will be further pursued by us in future research.

16. WHETHER ANY PH.D. ENROLLED/PRODUCED OUT OF THE PROJECT: **NO**(Student Support was not given)

17. NO. OF PUBLICATIONS OUT OF THE PROJECT .....07.....

( PLEASE ATTACH) – Attached

1. A. Mishra et.al. *Rapid photodegradation of methylene blue dye by rGO- V2O5 nano composite*, *J. Alloys and Compounds* (doi.org/10.1016/j.jallcom.2020.155746) (In Press) (I.F. 4.15)
2. A. Mishra, et.al. *Comparative electrochemical analysis of rGO-FeVO4 nanocomposite and FeVO4 for supercapacitor applications*, *App. Surf. Sci.* 488, 221(2019) (I.F.5.175)
3. G. Bera, et.al. *Multifunctionality of Partially Reduced Graphene Oxide –CrVO4 Nano-Composite: Electrochemical and Photocatalytic Studies with Theoretical Insight from Density Functional Theory*, *J. Phy. Chem C.* 122,21140 (2018) (I.F.4.37)
4. Ganesh Bera, et.al. *Triclinic – monoclinic – orthorhombic (T–M–O) structural transitions in phasediagram of FeVO4 -CrVO4 solid solutions*. *Journal of Applied Physics* 122(11):115101. (2017) (I.F. 2.10)
5. Priyanath Mal, et.al. *Electronic, magnetic and spectroscopic properties of doped Mn(1-x)AxWO4(A = Co, Cu, Ni and Fe) multiferroic: an experimental and DFT study*. *Journal of Physics Condensed Matter*, 29, 075901(2017) (I.F.2.657)
6. P.Rambabu et.al. *rGO- SnO2 Composites for Super capacitor Applications*, *IOP Conf. Series: Materials Science and Engineering* 149 (2016) 012169
7. P.Rambabu et.al. *Study of photocatalytic degradation of an industrial dye Ujala Supreme and Methyl Orange using SnO2 – rGO composites* *AIP Conf. Proceedings* 1728 (2016) 020375

  
( PRINCIPAL INVESTIGATOR )

**Dr. Goverdhan R. Turpu**  
Principal Investigator  
UGC MRP (F. No. 43-407 (2014) (SR))  
Department of Pure and Applied Physics  
Guru Ghasidas Vishwavidyalaya,  
Koni, Bilaspur (C.G.) 495009

  
(REGISTRAR/PRINCIPAL)

कुल सचिव/Registrar  
गुरु घासीदास विश्वविद्यालय, विलासपुर (छ.ग.)  
Guru Ghasidas Vishwavidyalaya,  
Bilaspur (C.G.) (Seal)

UNIVERSITY GRANTS COMMISSION  
BAHADUR SHAH ZAFAR MARG  
NEW DELHI – 110 002.


**Annual/Final Report of the work done on the Major Research Project. (Report  
to be submitted within 6 weeks after completion of each year)**

1. Project report No.: 1<sup>st</sup>/2<sup>nd</sup>/3<sup>rd</sup>/Final Final
2. UGC Reference No.F. 43-407/2014 (SR)
3. Period of report: from 01/07/2015 to 30/06/2018
4. Title of research project "Fabrication and characterization of Reduced graphene oxide Field Effect Transistors (rGO -FET) for sensor applications"
5. (a) Name of the Principal Investigator Dr. GOVERDHAN REDDY TURPU  
(b) Department. PURE AND APPLIED PHYSICS  
(c) University/College where work has progressed GURU GHASIDAS VISHWAVIDYALAYA
6. Effective date of starting of the project 01/07/2015
7. Grant approved and expenditure incurred during the period of the report:
  - a. Total amount approved Rs. 10,20,500.00
  - b. Total expenditure Rs. 79,344 =00 ✓
  - c. Report of the work done: (Please attach a separate sheet) (**Attached as Annexure A**)



SIGNATURE OF THE PRINCIPAL INVESTIGATOR

**Dr. Goverdhan R. Turpu**  
Principal Investigator  
UGC MRP (F. No. 43-407 (2014) (SR))  
Department of Pure and Applied Physics  
Guru Ghasidas Vishwavidyalaya,  
Koni, Bilaspur (C.G.) 495009

  
06.11.2020  
Registrar  
गुरु घासीदास विद्यालय, बिलासपुर (छ.ग.)  
Guru Ghasidas Vishwavidyalaya,  
Bilaspur (C.G.)

## 1. Objectives of the Project

- Synthesis of graphene oxide (GO) through modified hummer's method and reduction of GO to reduced graphene oxide (rGO) through chemical methods.
- Characterization of the GO and rGO through XRD, and Raman spectroscopic studies
- GO Film fabrication on Si/SiO<sub>2</sub> (300 nm) and patterning of GO film as a micro channel with the combination of photolithography and oxygen plasma etching
- Characterization of rGO – FETs using I – V characteristics and study adsorbate effects on electrical properties
- During Mid - term evaluation, the additional work related to photocatalytic and electrochemical applications of the composites of the rGO with functional materials was also discussed and presented.

## 2. Methodology

1. Synthesis of Graphene Oxide (GO) – standard modified Hummer's method
2. Characterization of graphene oxide through XRD and Raman studies
  - ✓ The X-Ray diffraction measurements are carried out using Rigaku Smart lab (9kW power, Cu  $k\alpha=1.54\text{\AA}$ ) in the  $2\theta$  range of  $10-80^\circ$ .
  - ✓ The Raman spectra were recorded in the region  $416-2000\text{ cm}^{-1}$  with Micro Raman spectrometer with model No. STR - 500, Cornes Technologies Ltd., Japan. The excitation wavelength of the laser used is 532.8 nm.
3. Fabrication of GO – thin films and patterning through photolithography and oxygen plasma etching
4. Reduction of thin films
5. Deposition of FET electrodes by evaporation method
6. Characterization through electrical measurements

## 3. Work done so far (please give details)

The work carried out so far in the project is classified as given below,

### A. Synthesis of Graphene Oxide and composites

**Materials:** For the synthesis of GO and its reduction the chemicals identified are natural graphite, sulfuric acid (H<sub>2</sub>SO<sub>4</sub>) (95–97%), hydrogen peroxide (H<sub>2</sub>O<sub>2</sub>) (30 wt.%), potassium permanganate (KMnO<sub>4</sub>), sodium nitrate (NaNO<sub>3</sub>), hydriodic acid (HI) (57 wt.%) and acetic acid. For cleaning and regular usage in the laboratory, methanol, isopropanol, nitric acid and membrane filter (200 nm) were used.

**Synthesis of graphene oxide (GO):** GO synthesis was done from natural graphite powder by the modified Hummers and Offenman's method [1] using sulfuric acid, potassium permanganate, and sodium nitrate.

**Synthesis of graphene oxide (rGO) – SnO<sub>2</sub> composites:** Reduced Graphene Oxide (rGO) - SnO<sub>2</sub> composite was prepared by mixing GO and SnO<sub>2</sub> precursor prepared by chemical solution methods. The SnO<sub>2</sub> precursor was prepared by adding 22.56 gm of SnCl<sub>2</sub>·2H<sub>2</sub>O to 100 ml absolute ethanol (1M solution) and stirred at 60°C for 30 min in a closed vessel to obtain the clear, transparent and homogeneous solution. 9.496 ml of GO was added to 40 ml Tin Chloride solution in a closed vessel and the admixture was stirred at 80°C for 1h. The obtained powder after drying was washed with de- ionized water several times and finally with ethanol 2-3 times and dried at 100°C in the oven for 24 hours. rGO- SnO<sub>2</sub> composite powders were annealed at 500°C temperatures in inert ambient. SnO<sub>2</sub> was prepared through similar method without GO addition.

**Synthesis of graphene oxide (rGO) – Orthovanadate composites:** Further, recently composites with various photocatalytic materials like FeVO<sub>4</sub>, CrVO<sub>4</sub> and BiVO<sub>4</sub> are also synthesized through ultrasonication method to study the photocatalytic and electrochemical applications.

## B. Characterization of Graphene Oxide and Composites through XRD and Raman Studies

### a) XRD and Raman Studies of GO and rGO-SnO<sub>2</sub>:

The figure 1(a) shows that the X-Ray diffraction patterns of GO and rGO-SnO<sub>2</sub> samples. The obtained reflections for SnO<sub>2</sub> indicate the tetragonal rutile phase of SnO<sub>2</sub> matching with JCPDS Card No. 41-1445 [1]. Further, the rGO-SnO<sub>2</sub> composites also exist in the same phase. The peak corresponding with GO was not observed in rGO-SnO<sub>2</sub>. This may be due to the less amount of GO in the composite and dominating strong intensity peaks of SnO<sub>2</sub> [2]. The XRD pattern of GO with 2θ value 11.11° corresponding to (002) reflection with interlayer d-spacing 7.96Å indicates the successful preparation of GO by oxidation of Graphite [3].

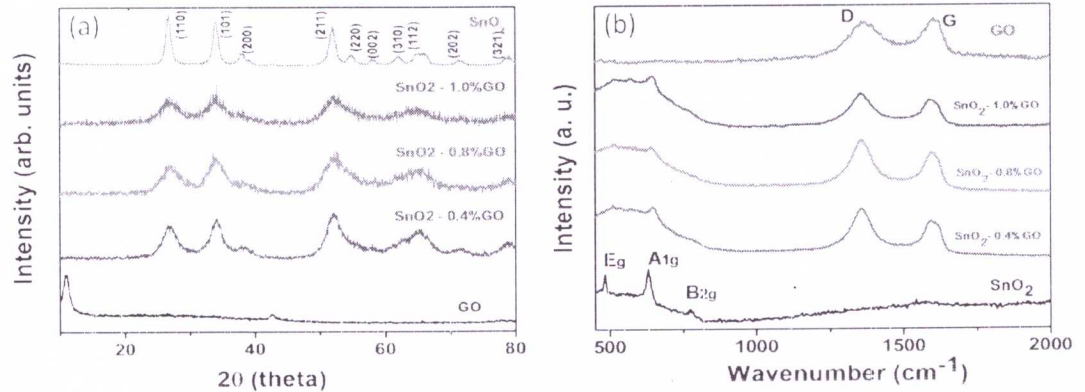


Figure 1(a) X-ray diffraction pattern of GO, SnO<sub>2</sub> and SnO<sub>2</sub> - rGO composites; (b) Raman spectra of GO, SnO<sub>2</sub> and SnO<sub>2</sub> - rGO composites.

The figure 1(b) shows the Raman spectra of GO and rGO-SnO<sub>2</sub> samples. From The peaks at 485.1 cm<sup>-1</sup>, 631.3 cm<sup>-1</sup> and 771.1 cm<sup>-1</sup> corresponds to the E<sub>g</sub>, A<sub>1g</sub> and B<sub>2g</sub> vibration modes of SnO<sub>2</sub> respectively [4]. The degree of disorder and the average size of sp<sup>2</sup> domains are measured in terms of ID/IG ratio [5]. The value of ID/IG ratio for composites is greater than that of GO due to the formation of sp<sup>2</sup> domains and indicates that GO was reduced due to the addition of Sn during the reaction [6].

### b) XRD and Raman Studies of GO and rGO-CrVO<sub>4</sub>:

Figure 2(a) shows the XRD pattern of GO, CrVO<sub>4</sub>, and rGO-CrVO<sub>4</sub> composite. The diffraction peak indicating (001) plane of GO corresponds to the interlayer space (d spacing) of 0.75 nm, which is larger than the d spacing of natural graphite (0.34 nm) [7]. The XRD pattern of CrVO<sub>4</sub> shows pure single-phase formation of the compound and is indexed to the orthorhombic structure having Cmc<sub>2</sub>m space group. The lattice parameters evaluated by Rietveld analysis for CrVO<sub>4</sub> are a = 5.5818 Å, b = 8.2390 Å, and c = 5.9953 Å [8]. The prepared composite of rGO and CrVO<sub>4</sub> shows the peaks corresponding to both rGO and CrVO<sub>4</sub>, indicating the formation of rGO-CrVO<sub>4</sub> composite successfully. It is also observed that the peak corresponding to (001) plane of GO shifts toward the higher angles indicating the reduction of the GO by adding CrVO<sub>4</sub> to it. It is evident that the materials prepared are pure and are in single-phase from the XRD studies. Figure 2(b) shows the Raman spectra of GO, CrVO<sub>4</sub>, and rGO-CrVO<sub>4</sub> composite. The main features in the Raman spectra of graphitic carbon-based materials are the G and D peaks and their overtones. The first-order G and D peaks, both arising from the vibrations of sp<sup>2</sup> carbon, appear around 1570 and 1354 cm<sup>-1</sup>, respectively [9]. The G peak corresponds to the optical E<sub>2g</sub><sup>-1</sup> phonons at the Brillouin zone center, resulting from the bond stretching of sp<sup>2</sup> carbon pairs in both rings and chains. The D peak represents the breathing mode of aromatic rings arising because of the defect in the sample. The D-peak intensity is therefore often used as a measure for the degree of disorder. The Raman spectra of GO shows the G and D bands at 1583.27 and 1345 cm<sup>-1</sup>, respectively, with the intensity ratio between D and G peaks, ID/IG = 1.04. CrVO<sub>4</sub> having orthorhombic crystal structure with Cmc<sub>2</sub>m space group has four symmetry inequivalent atoms in the unit cell occupying 4a, 4c, 8f, and 8g positions. The group theory analysis predicts the following irreducible representation at Γ point: Γ = 5A<sub>g</sub> + 4B<sub>1g</sub> + 6B<sub>1u</sub> + 3A<sub>u</sub> + 2B<sub>2g</sub> + 7B<sub>2u</sub> + 4B<sub>3g</sub> + 5B<sub>3u</sub>; out of these 36 phonon modes, there exist three acoustic modes (B<sub>1u</sub>, B<sub>2u</sub>, and B<sub>3u</sub>),

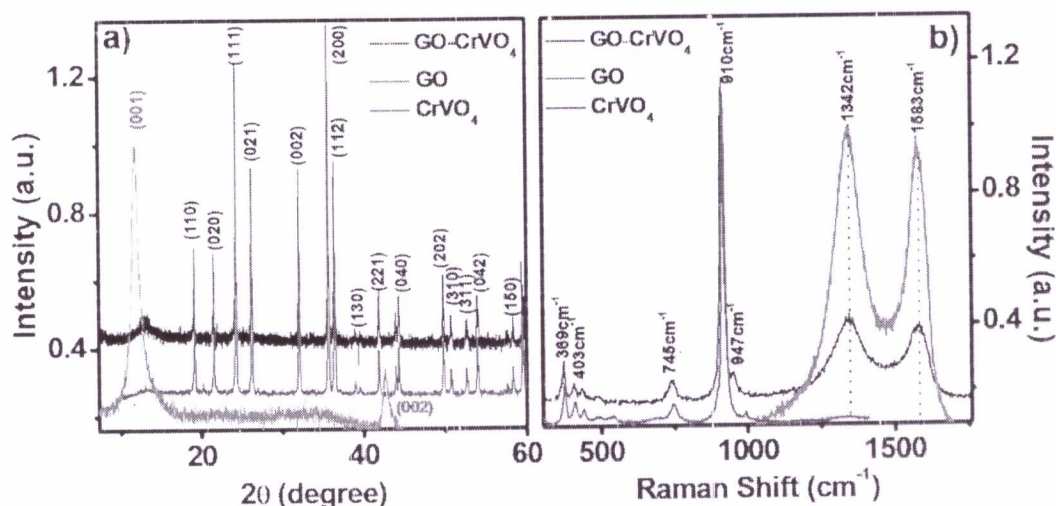


Figure 2 (a) XRD patterns and (b) Raman spectra of  $\text{CrVO}_4$  (blue line),  $\text{rGO}$  (red line), and  $\text{rGO-CrVO}_4$  composite (black line), respectively.

three silent modes (Au), 15 infrared (IR) modes (5B1u, 6B2u, and 4B3u), and 15 Raman active modes (5Ag, 4B1g, 2B2g, and 4B3g). Raman active vibrational modes can be classified as internal and external modes of the  $\text{VO}_4$  units [10]. The modes at high frequency ( $900\text{ cm}^{-1}$ ) are internal modes of  $\text{VO}_4$  tetrahedra because of symmetric and asymmetric stretching and bending. The modes at lower wave number are due to pre-translational (T) and modes in between these two are due to pure rotational (R) modes. The Raman spectra of composite material ( $\text{rGO-CrVO}_4$ ) show all modes as observed in the pristine compounds with a slight shift toward the lower wave numbers. The intensity ratio of D and G peaks of  $\text{rGO}$  in the composite changes to 1.09–1.04, indicating possible partial reduction of GO into  $\text{rGO}$  [11] because of the formation of bonds on the  $\text{rGO}$  sheet with Cr/V ions.

### c) XRD and Raman Studies of GO, $\text{FeVO}_4$ and $\text{rGO-FeVO}_4$ :

Fig. 3 shows the XRD patterns of  $\text{FeVO}_4$ , GO and  $\text{rGO-FeVO}_4$ . The XRD of graphene oxide was recorded in the  $2\theta$  range

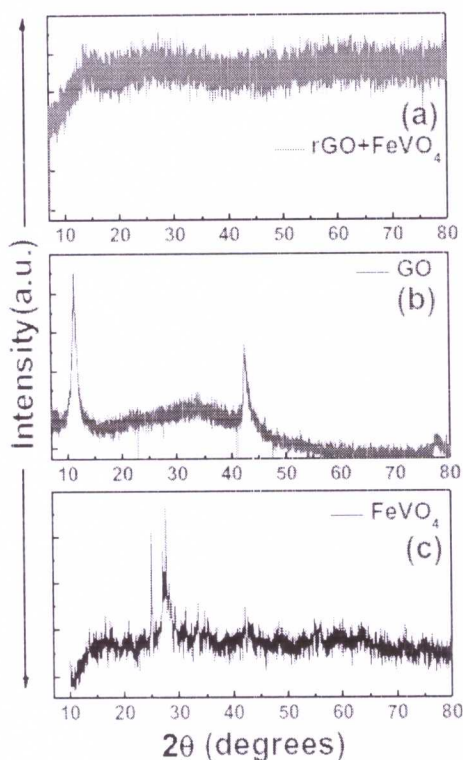


Figure 3 X-ray diffraction pattern of graphene oxide (a)  $\text{rGO-FeVO}_4$ , (b) GO and (c)  $\text{FeVO}_4$ .

between  $8^\circ$ – $80^\circ$  which shows a (002) diffraction peak at  $2\theta=11.12^\circ$  and (001) diffraction peak at  $2\theta=42.67^\circ$  [12]. XRD Spectra of  $\text{FeVO}_4$  is measured in range between  $10^\circ$ – $80^\circ$  where the XRD spectra confirms that  $\text{FeVO}_4$  is pure and is in triclinic phase [13, 14]. The XRD pattern of  $\text{FeVO}_4$  manifests broad peaks indicating particle sizes in nano range ( $\sim 39\text{ nm}$ ). Due to low temperature synthesis of the compound it is expected that the nanoparticles possess poor crystallinity when compared to compounds annealed at higher temperatures [15]. The same is observed in terms of lesser counts in XRD pattern and fewer Bragg's peaks with broad nature as compared to bulk  $\text{FeVO}_4$  [10]. The XRD of  $\text{rGO-FeVO}_4$  shows a broad hump around  $2\theta$  values of  $25^\circ$  indicating poor crystalline nature or nearly amorphous behavior. This broad hump is due to the overlap of  $\text{rGO}$  and  $\text{FeVO}_4$  characteristic peaks appearing at approximately same angles. The absence of sharp peaks is due to poorly crystalline nano particles of  $\text{FeVO}_4$  and diffused XRD behavior of  $\text{rGO}$ . Further we want to mention that GO and  $\text{FeVO}_4$  were taken in 1:1 ratio.

Fig. 4 shows the Raman spectra of GO,  $\text{FeVO}_4$  and  $\text{rGO-FeVO}_4$  samples. The characteristic spectra of graphitic carbon material D and G peaks which arise due to the vibration of  $\text{sp}^2$  hybridized carbon in ring

and chain. The D band corresponds to the disorder in the aromatic ring because of the breathing of  $sp^2$  and  $sp^3$  hybridized carbons in the ring. The G band corresponds to the bond stretching of  $sp^2$  carbons in the ring and chain [16, 17]. In our sample the G and D peaks appear at  $1578.92\text{ cm}^{-1}$  and  $1343.55\text{ cm}^{-1}$  respectively.  $\text{FeVO}_4$  having triclinic structure (P-1 space group and atoms at 2i positions) contains three symmetry inequivalent  $\text{Fe}^{3+}$  sites and three symmetry inequivalent  $\text{V}^{5+}$

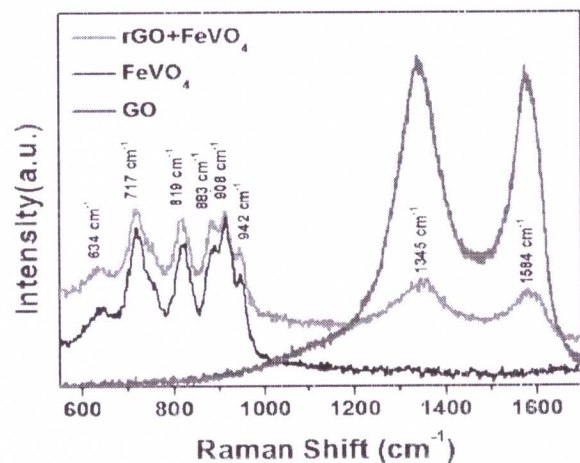


Figure 4 Raman spectra of graphene oxide (GO),  $\text{FeVO}_4$  and rGO- $\text{FeVO}_4$  nanocomposite.

ions in the unit cell which forms two  $\text{FeO}_6$  octahedrons, one  $\text{FeO}_5$  polyhedron (trigonal bipyramidal), and three  $\text{VO}_4$  tetrahedron [18]. The polyhedrons are linked with oxygen atoms at vertices. The primitive cell of  $\text{FeVO}_4$  contains 36 atoms and in principle 108 vibrational modes are expected. According to the group theory analysis, the irreducible representation at  $\Gamma$  point is  $\Gamma=54\text{Ag}+54\text{Au}$  among which 54 optical modes are Raman active (Ag), 51 are infrared active (Au), and 3 (Au) modes are acoustic modes [10]. The spectra of  $\text{FeVO}_4$  contains distinct peaks which appears majorly because of V-O-Fe stretching where the peaks at higher wave numbers are due to the V-O stretching and the peaks at lower frequencies ( $\leq 500\text{ cm}^{-1}$ ) are due to relative torsional motion between polyhedrons [19]. In rGO- $\text{FeVO}_4$  the characteristic peaks of graphene oxide and triclinic  $\text{FeVO}_4$  coexists in the Raman spectra. The ID/IG ratio decreases from 0.96 to 0.92 in composite material compared to GO indicating the increase in ordering of  $sp^2$  bonded graphitic domains suggesting reduction of GO to rGO.

### C. Photocatalytic studies

#### a) Photocatalytic studies of rGO – $\text{SnO}_2$ :

Photocatalytic activity of  $\text{SnO}_2$  and  $\text{SnO}_2$  - 1% rGO composites in the degradation of two organic dyes, Methyl Orange (MO) and Ujala Supreme (US) (a fabric whitener) is studied. Ujala Supreme (US) is a synthetic organic colouring agent which is diluted form of acid violet paste and is very similar to the organic compound Acid-Violet-49. The chemical structures of Methyl Orange and Acid-Violet-49 are as shown below. Figure 5. shows UV – Vis spectra of a) US in 1% rGO –  $\text{SnO}_2$ , b) US in  $\text{SnO}_2$ , c) MO with time and in  $\text{SnO}_2$  and d) MO in 1% rGO –  $\text{SnO}_2$  in progressive intervals of times upto 180 min. The solution prepared was kept in dark conditions to complete these time dependent measurements. The time dependent UV-Vis spectra of US in  $\text{SnO}_2$  show gradual reduction in absorption intensity of the dye as evidenced by Figure 4b whereas, in presence of  $\text{SnO}_2$ -rGO composite the reduction occurs faster compared to the  $\text{SnO}_2$  solutions. The reduction in absorption intensity can be understood in terms of the degradation of dye.

The photo catalytic reaction mechanism of  $\text{SnO}_2$  can be understood in the following way: when photo catalyst  $\text{SnO}_2$  is excited via UV radiation having greater energy than its band gap energy, the electron - hole pair is generated in the  $\text{SnO}_2$  and subsequently, redox reactions occur and form superoxide ions ( $\text{O}_2^-$ ) and hydroxyl radicals ( $\text{OH}^-/\text{OH}\cdot$ ) which are strong oxidizing agents and can react with the dye molecules in favour of its degradation directly. The dye molecule can therefore interact with the photo generated holes in the valence band (VB), and provides a direct chemical reaction between the dye and the photo catalyst [20]. Further, the incorporation of rGO over  $\text{SnO}_2$  nano particles was made assuming that rGO could offer enhanced photo catalytic activity due to its exceptional electrical conductivity and extremely efficient absorption which promotes the adsorption of organic molecules and inhibits the electron-hole recombination. The photo catalytic activity of  $\text{SnO}_2$  and  $\text{SnO}_2$ -rGO composite on MO and US shows similar effects resulting in faster degradation due to the incorporation of rGO in the composites.



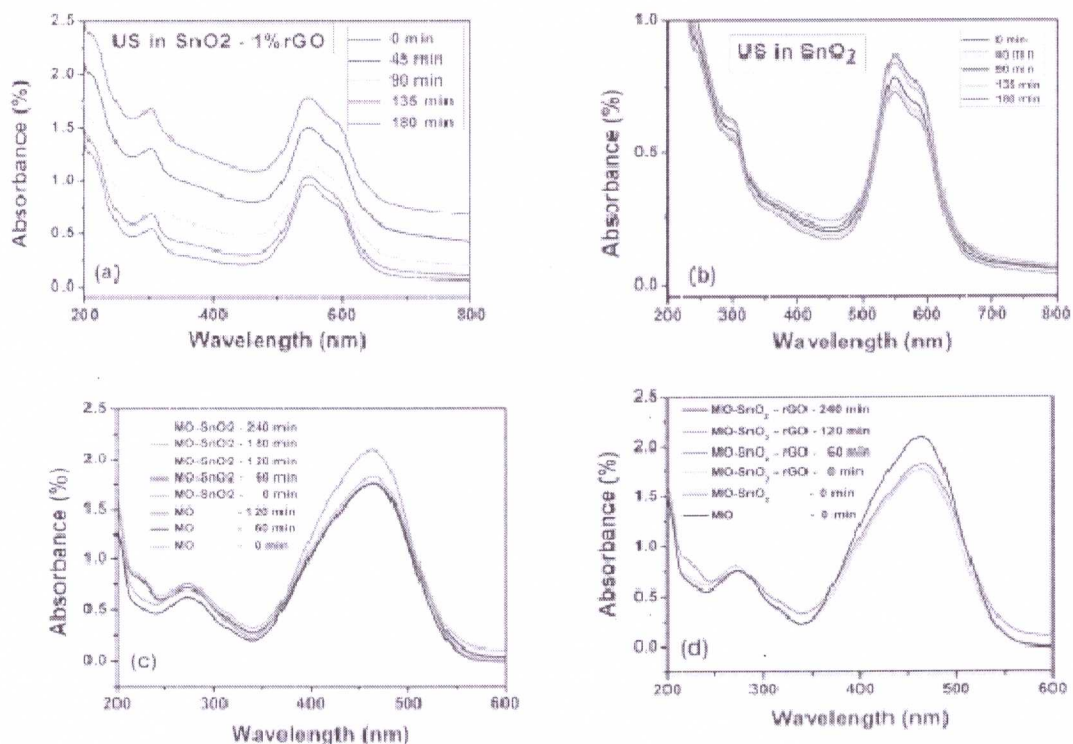


Figure 5 UV – vis absorbance spectra of the solutions kept in dark conditions (0 - 180 min with 45 min interval) a) US in 1% rGO - SnO<sub>2</sub>, b) SnO<sub>2</sub>, c) MO in SnO<sub>2</sub> and d) MO in 1% rGO - SnO<sub>2</sub>.

#### b) Photocatalytic studies of CrVO<sub>4</sub> and rGO – CrVO<sub>4</sub>:

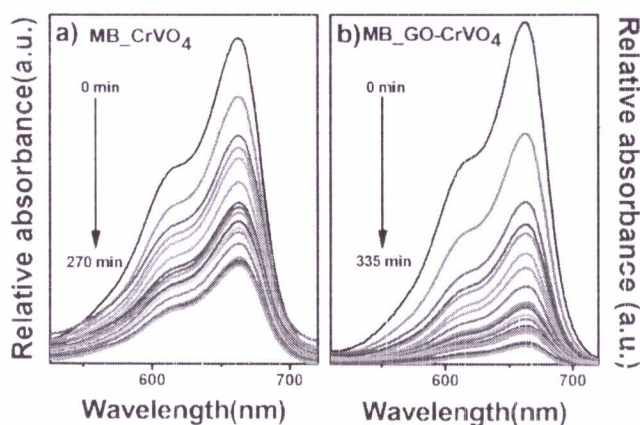


Figure 6 UV-visible absorbance spectra of MB dye solution with performance of (a) CrVO<sub>4</sub> and (b) rGO-CrVO<sub>4</sub> composite.

The photocatalytic degradation process obeys the first-order decay kinetics as represented in Figure 7(b), and the rate constants were estimated according to the following formula [22];

$$C_t = C_0 \exp(-kt); \text{ or, } \ln C_0/C_t = kt$$

where,  $C_0$  is the initial concentration of dye solution (mol/L),  $C_t$  is the concentration of the dye at various interval times (mol/L),  $t$  is the illumination time, and  $k$  is the reaction rate constant. The evaluated rate constants are 0.0332 and 0.0670 min<sup>-1</sup> for CrVO<sub>4</sub> and rGO-CrVO<sub>4</sub> composite catalysts, respectively. It is evident that the composite has almost twofold photocatalytic activity as compared to CrVO<sub>4</sub>. This increase suggests that there is a synergistic effect between rGO and CrVO<sub>4</sub>.

Figure 6(a,b) displays the intensity of absorption spectra of MB dye which is having a maximum absorbance at 668 nm and is gradually decreasing on increasing the irradiation time to 330 and 400 min for CrVO<sub>4</sub> and rGO-CrVO<sub>4</sub> composite, respectively. The maximal position of absorption is not altered during the removal process indicating the complete destruction of the dye pollutant into inorganic carbon, and no other intermediate organic products are formed in the degradation process [21]

Figure 7(a) shows the degradation of initial concentration of MB dye with respect to time. The photocatalytic

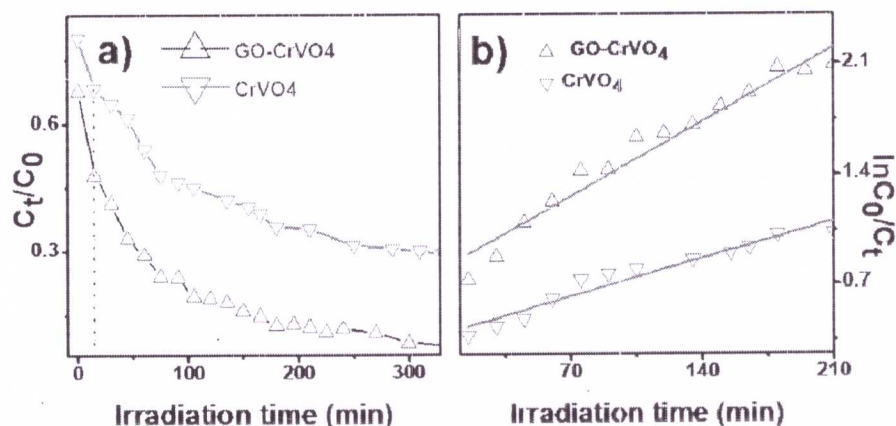


Figure 7 (a) Photodegradation reaction efficiency of MB solution using  $\text{CrVO}_4$  and  $\text{rGO-CrVO}_4$  composite (b) first-order kinetic linear fitting curves of MB photocatalytic degradation with same catalysts.

## D. Electrochemical studies

### a) Electrochemical studies of $\text{rGO-SnO}_2$

The cyclic voltammetric studies for  $\text{SnO}_2$  and  $\text{rGO-SnO}_2$  composite have been recorded in the potential range of  $-0.8-0.8\text{V}$  with a scan rate of  $1\text{ mV/sec}$  in  $0.5\text{M H}_2\text{SO}_4$  solution. Figure 8(a) shows the voltammograms of  $\text{rGO-SnO}_2$  in two different scan rates of  $0.1$  and  $0.03\text{ V/s}$  and 8(b) shows half cycle in the range of  $-8-0\text{ V}$  with two different scan rates  $0.01$  and  $0.03\text{ V/s}$ . Figure 8(c) shows voltammograms of  $\text{SnO}_2$  with different scan rates between  $0.5$  to  $0.05\text{ V/s}$ . Fig. 8(d) shows the comparative curves for both  $\text{rGO-SnO}_2$  and  $\text{SnO}_2$  where the increase in the area of the voltammogram is greater for composite material at a given scan rate and range. As can be observed from the graphs, the CV curves deviate from the rectangular shape and get distorted. This distortion increases with the change in the scan rate. This can be due to the polarization [23].

The specific capacitance of the both samples was found using the formula:

$$C = \int i(E)dE / (2mv (E_2 - E_1))$$

where  $C$  is capacitance (in farad (F)),  $i(E)$  is the instantaneous current (in A),  $\int i(E)dE$  is the total voltammetric charge obtained by integration of positive and negative sweep in CV,  $m$  is the mass (in gm),  $v$  is the scan rate (in V/sec) and  $(E_2-E_1)$  is the potential window width (in V).

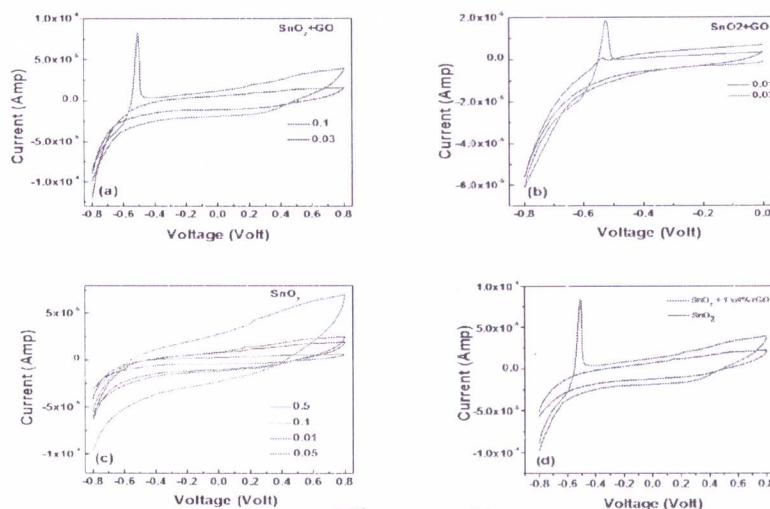


Figure 8 Cyclic Voltammograms of a)  $1\% \text{ rGO-SnO}_2$  in the range of  $-0.8-0.8\text{ V}$  with scan rates of  $0.1$  and  $0.03\text{ V/s}$ , b)  $1\% \text{ rGO-SnO}_2$  in the range of  $-0.8-0\text{ V}$  with scan rates of  $0.01$  and  $0.03\text{ V/s}$ , c)  $\text{SnO}_2$  in the range of  $-0.8-0.8\text{ V}$  with scan rates of  $0.05, 0.01, 0.1$  and  $0.5\text{ V/s}$  and d) comparative cycles of  $1\% \text{ rGO-SnO}_2$  and  $\text{SnO}_2$  in the range of  $-0.8-0.8\text{ V}$  with scan rates of  $0.1\text{ V/s}$

From the Figure 8(d), it is evident that the area of the composite curve is more compared to the pure SnO<sub>2</sub> which clearly indicates that the rGO-SnO<sub>2</sub> composite is having more specific capacitance (4.66 F/gm) than that of pure SnO<sub>2</sub> (2.86 F/gm). Here the specific capacitance of the composite is 1.62 times higher than that of pure SnO<sub>2</sub>. So the composite can be used in super capacitor applications since the addition of GO to the SnO<sub>2</sub> enhances its capacitive behaviour [24].

From the electrochemical impedance measurements, Nyquist plots of the Pure SnO<sub>2</sub> and rGO-SnO<sub>2</sub> composite samples

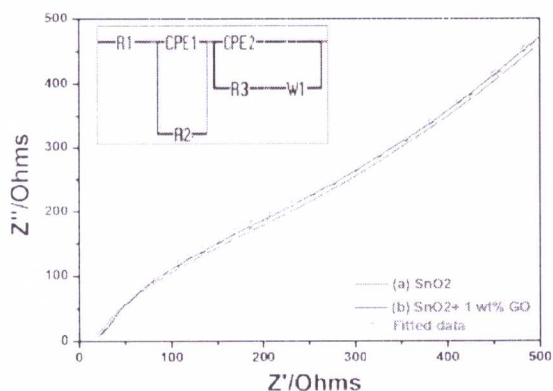


Figure 9 Nyquist plots of (a) SnO<sub>2</sub> and (b) SnO<sub>2</sub> + 1wt% rGO, inset showing equivalent circuit.

were shown in the Figure 9. Accordingly, an equivalent circuit matching the electrochemical behaviour of the samples was simulated [25], as shown in the inset of Fig. 9. The circuit elements are composed of bulk solution resistance (R1) which is the solution resistance between working electrode and reference electrode, the high frequency semicircle is associated with SEI film resistance (R2), the middle frequency semicircle is linked to charge-transfer resistance through the electrode-electrolyte interface (R3), CPE1 and CPE2 are the constant phase elements and the inclined line is associated with the Warburg impedance W<sub>1</sub> [26]. The diameters of high and low frequency regions give the SEI resistance (R2) and Charge transfer resistance (R3) directly.

Table 1: Bulk solution resistance (R1), Solid Electrolyte Interface resistance (R2), and Charge transfer resistance (R3) values obtained through the fitting to Nyquist plots of SnO<sub>2</sub> and SnO<sub>2</sub> + 1wt% rGO

Sample	R1 (in Ohm)	R2 (in Ohm)	R3 (in Ohm)
SnO <sub>2</sub>	17.1	178	70902
SnO <sub>2</sub> – 1%rGO	17.9	168	44577

From the Table 1, it can be seen that the diameters of the semicircles in the high and low frequency regions for the rGO-SnO<sub>2</sub> composite are lower than that of pure SnO<sub>2</sub>. The obtained parameters after fitting tell that the value of the charge transfer resistance R3 for the composite is much lower than that of the Pure SnO<sub>2</sub> which clearly indicates that improvement of the charge transfer performance of the composite. Also the value of the SEI film resistance R2 for the composite is lower than that of the Pure SnO<sub>2</sub> which obviously reveals the high conductivity of the composite than that of pure SnO<sub>2</sub>. Therefore, the presence of GO in SnO<sub>2</sub> not only enhances the conductivity of the composite but also largely enhances the electrochemical activity of SnO<sub>2</sub>.

#### b) Electrochemical studies of rGO – CrVO<sub>4</sub>:

Figure 10(a,b) shows the cyclic voltammograms of CrVO<sub>4</sub> and rGO-CrVO<sub>4</sub> composite at different scan rates. The CrVO<sub>4</sub> cyclic voltammogram shows various oxidative and reduction peaks, whereas in composite material, these peaks almost disappeared. The composite CV shows a nearly rectangular shape, which are typical for an electrical double-layer capacitive behavior. A gradual increase in the current with the increase in the scan rate is also observed. Notably, at the scan rate of 20 mV/s, the behavior can be compared with other high-power SCs found in literature. Figure 8c shows a comparison between CrVO<sub>4</sub> and rGO-CrVO<sub>4</sub> at 5 mV/s, the three redox peaks appearing in CV of CrVO<sub>4</sub> at -0.2768, 0.3302, 0.7377 V in the anodic sweep and three peaks -0.7138, -0.3284, and 0.3421 V in the cathodic sweep get disappeared in rGO-CrVO<sub>4</sub> composite. Nearly a three times increase in capacitance is observed for composite in contrast to CrVO<sub>4</sub> largely because of the increase in the surface area of the composite and availability of various conduction paths in rGO.

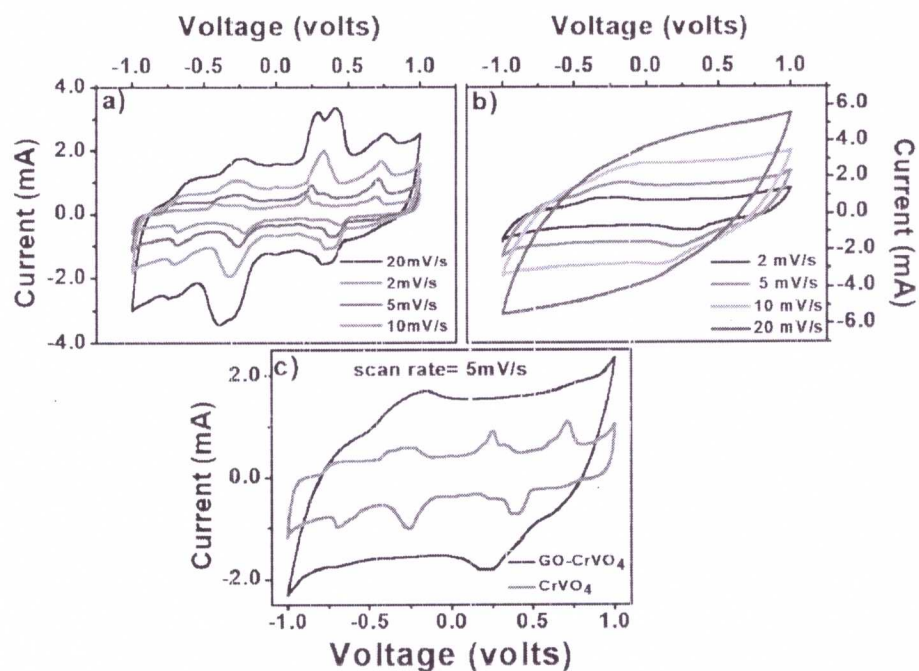


Figure 10 Cyclic voltammograms of (a) CrVO<sub>4</sub> and (b) rGO-CrVO<sub>4</sub> composite at different scan rates and (c) a comparison between CrVO<sub>4</sub> and rGO-CrVO<sub>4</sub> at 5 mV/s.

Figure 11(a,b) shows the galvanometric charging discharging (GCD) curve of CrVO<sub>4</sub> and rGO-CrVO<sub>4</sub> composite at different current densities of 0.5, 1.0, 5.0, and 10.0 mA/cm<sup>2</sup>, respectively. Therefore, triangular shapes were observed for GCD curves at different current densities. The calculated specific capacitance of rGO-CrVO<sub>4</sub> composite is 102.66 F/g for  $4.45 \times 10^{-3}$  g of electrode material and that of CrVO<sub>4</sub> is 30.87 F/g at a scan rate of 0.5 mA/cm<sup>2</sup>. The discharge curve of rGO-CrVO<sub>4</sub> is quite linear as compared to CrVO<sub>4</sub>, with a minimal IR drop visible at the start of each discharge curve. At higher scan rates, the IR drop becomes more visible. Figure 12 shows a Nyquist curve of rGO-CrVO<sub>4</sub> composite in the frequency range of 100 KHz to 10mHz, where there is an internal resistance  $R_s = 9.64 \Omega$  in the high-frequency region; on the other hand, the  $R_s$  in CrVO<sub>4</sub> was 15.91  $\Omega$ .

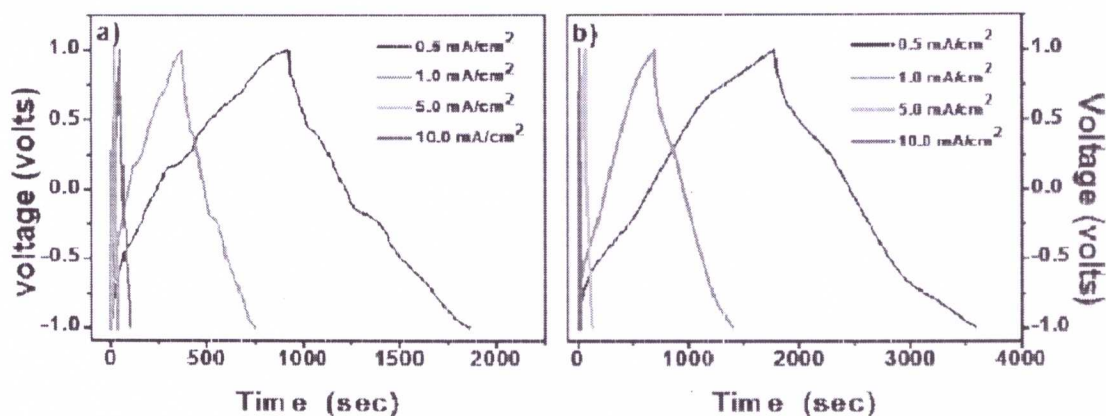


Figure 11 GCD curve of (a) CrVO<sub>4</sub> and (b) rGO-CrVO<sub>4</sub> composite at different current densities.

The partial semicircle in the high-frequency to mid-frequency region is modeled by an interfacial charge-transfer resistance  $R_{ct} = 0.854 \Omega$ ; on the other hand, the  $R_{ct}$  of CrVO<sub>4</sub> was 14.87  $\Omega$ . A low  $R_s$  and  $R_{ct}$  of rGO-CrVO<sub>4</sub>, respectively, in the high-frequency region is attributed to balanced electronic and ionic conduction in composite material. Moreover, the impedance curve of composite parallel to the imaginary axis indicates the capacitive nature of rGO-CrVO<sub>4</sub> composite. The high  $R_s$  and  $R_{ct}$  for CrVO<sub>4</sub> indicate high diffusion resistance and resistive electron-transfer pathways. This substantially differentiates CrVO<sub>4</sub> and rGO-CrVO<sub>4</sub> in turn which holds larger charge storage capacity [27].

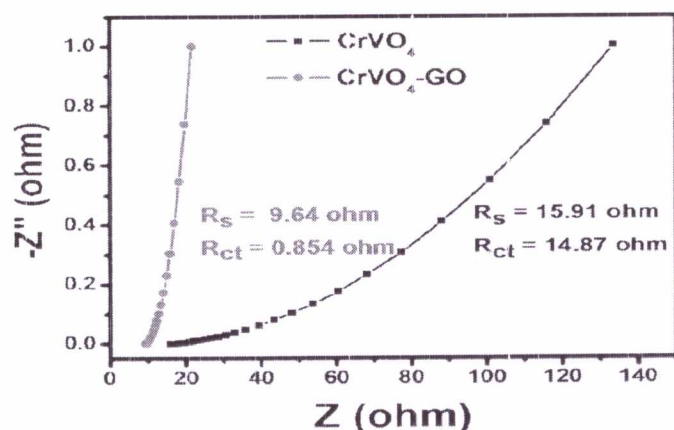


Figure 12 Nyquist curve of  $\text{CrVO}_4$  (black) and  $\text{rGO-CrVO}_4$  (red) in the frequency range of 100 KHz to 10 mHz.

### e) Electrochemical studies of $\text{rGO-FeVO}_4$ :

Fig. 13(a) & (d) shows the Cyclic Voltammograms of  $\text{FeVO}_4$  and  $\text{rGO-FeVO}_4$  composite material taken in a voltage window from  $-1.0$  to  $1.0$  at  $5 \text{ mV/s}$ ,  $10 \text{ mV/s}$  and  $20 \text{ mV/s}$  sweep rates. In  $\text{FeVO}_4$  sharper oxidation peaks at  $-0.00929 \text{ V}$ ,  $0.7481 \text{ V}$  and  $0.9944 \text{ V}$  on anodic sweep and reduction peaks at  $0.4730 \text{ V}$ ,  $-0.6778 \text{ V}$  and  $-0.9926 \text{ V}$  on cathodic sweep were observed and are due to two redox couples  $\text{Fe}^{3+}/\text{Fe}^{2+}$  and  $\text{V}^{5+}/\text{V}^{4+}$  [28]. Whereas in  $\text{rGO-FeVO}_4$  composite intensity of the peaks is reduced may be due addition of graphene oxide there will be an insertion of  $\text{FeVO}_4$  into the layer of graphene oxide resulting in the overlapping of redox peaks of redox couples. Fig. 13(b) & (e) shows the Galvanometric charging discharging curve of  $\text{FeVO}_4$  and  $\text{rGO-FeVO}_4$  composite at different current densities i.e.  $0.5 \text{ mA/cm}^2$ ,  $1 \text{ mA/cm}^2$ ,  $5 \text{ mA/cm}^2$  up to  $10 \text{ mA/cm}^2$ . The humps appearing on the charging and discharging curve of  $\text{FeVO}_4$  at  $0.5 \text{ mA/cm}^2$  matches well with the cyclic voltammogram, whereas the humps nearly get disappeared in the charging and discharging curve of  $\text{rGO-FeVO}_4$  at  $0.5 \text{ mA/cm}^2$ . The specific capacitances evaluated by using GCD curve for  $\text{FeVO}_4$  and  $\text{rGO-FeVO}_4$  are  $97.54 \text{ g/F}$  and  $189.10 \text{ g/F}$ , respectively. The specific capacitance increases drastically (all most double) by the addition of GO to  $\text{FeVO}_4$ . The IR drop appearing in the beginning of discharging curve of  $\text{FeVO}_4$  at  $0.5 \text{ mA/cm}^2$  gets reduced in  $\text{rGO-FeVO}_4$  at  $0.5 \text{ mA/cm}^2$  indicating a good characteristic of  $\text{rGO-FeVO}_4$  as a supercapacitor.

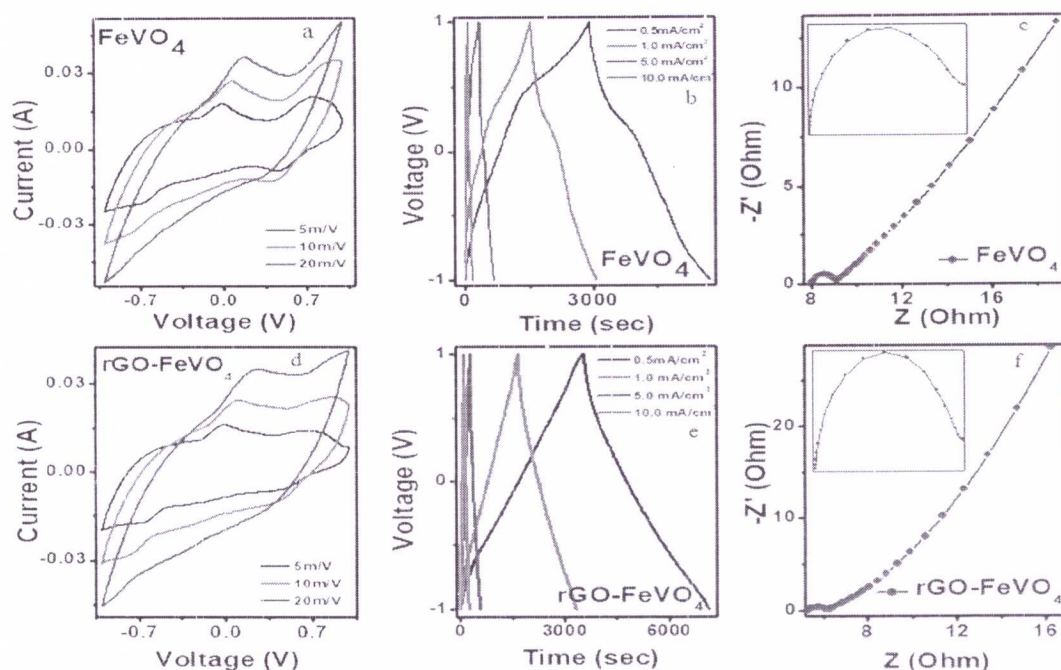


Figure 13 Cyclic voltammogram curve of a)  $\text{FeVO}_4$  and d)  $\text{rGO-FeVO}_4$  in voltage window of  $-1.0 \text{ V}$  to  $1.0 \text{ V}$  at  $5 \text{ mV/s}$ ,  $10 \text{ mV/s}$  and  $20 \text{ mV/s}$  swipe rate; galvanometric charging discharging curve of b)  $\text{FeVO}_4$  and e)  $\text{rGO-FeVO}_4$  and the Nyquist plot of c)  $\text{FeVO}_4$  and f)  $\text{rGO-FeVO}_4$ .

Fig. 13(c) & (f) shows the Nyquist curve of FeVO<sub>4</sub> and rGO-FeVO<sub>4</sub> in 100 kHz to 10 mHz frequency range. As it can be seen the Nyquist curve shows a semicircle in the higher frequency range followed by a slanted line in the lower frequency range. The semicircle formation indicates that there is small/lower charge transfer resistance between electrolyte and electrode [29]. rGO-FeVO<sub>4</sub> possess smaller impedance arc radius which means it possess lower charge transfer resistance and higher electron mobility compared to FeVO<sub>4</sub>. This could be due to the increase in the effective surface area which is beneficial for higher electron conduction [30]. The R<sub>s</sub> and R<sub>ct</sub> values measured by Nyquist plot of FeVO<sub>4</sub> and rGO-FeVO<sub>4</sub> are 8.02 Ω, 0.975 Ω and 6.17 Ω, 0.829 Ω respectively.

## References

- Mrcano, D. C.; Kosynkin, D. V.; Berlin, J. M.; Sinitskii, A.; Sun, Z.; Slesarev, A.; Alemany, L. B.; Lu, W.; Tour, J. M. *ACS Nano* 2010, **4**, 4806–4814.
- H. Seema, K. C. Kemp, V. Chandra and K. S. Kim, *Nanotechnology* **23**, 355705 (2012).
- S. Dubin, S. Gilje, K. Wang, V.C. Tung, K. Cha, A.S. Hall, J. Farrar, R. Varshneya, Y. Yang, R.B. Kaner, *ACS Nano* **4**, 3845 (2010).
- A. Leonardy, W-Z Hung, D-S Tsai, C-C Chou and Y-S Huang, **9**, 3958 (2009).
- B. Zhao, G. Zhang, J. Song, Y. Jiang, H. Zhuang, P. Liu, T. Fang, *Electrochimica Acta* **56**, 7340 (2011).
- M. Chen, C. Zhang, L.Li, Y. Liu, X. Li, X. Xu, F. Xia, W. Wang, and J. Gao, *ACS Appl. Mater. Interfaces* **5**, 13333 (2013).
- Paulchamy, B.; Arthi, G.; Lignesh, B. D., *J. Nanomed. Nanotechnol.* 2015, **6**, 253.
- Baran, E. J., *J. Mater. Sci.* 1998, **33**, 2479–2497.
- Krishnamoorthy, K.; Veerapandian, M.; Yun, K.; Kim, S.-J, *Carbon* 2013, **53**, 38–49.
- Bera, G.; Reddy, V. R.; Rambabu, P.; Mal, P.; Das, P.; Mohapatra, N.; Padmaja, G.; Turpu, G. R., *J. Appl. Phys.* 2017, **122**, 115101.
- Fu, C.; Zhao, G.; Zhang, H.; Li, S., *Int. J. Electrochem. Sci.* 2013, **8**, 6269–6280.
- L. Stobinski, B. Lesiaka, A. Malolepszy, M. Mazurkiewicz, B. Mierzwa, J. Zemek, P. Jiricek, I. Bieloshapka, *J. Electron Spectrosc. Relat. Phenom.* 195 (2014) 145–154.
- S. Moreno, D. Errandonea, J. Porres, D. García, S.J. Patwe, S.N. Achary, A.K. Tyagi, P.R. Hernández, A. Muñoz, C. Popescu, *Inorg. Chem.* **57** (2018) 7860–7876.
- Y. Zhao, K. Yao, Q. Cai, Z. Shi, M. Sheng, H. Lina, M. Shao, *Cryst. Eng. Comm.* **16** (2014) 270.
- G. Bera, S. Sinha, P. Rambabu, P. Das, A.K. Gupta, G.R. Turpu, *AIP Conference Proceedings* 1728 (2016) 020284.
- D.R. Dreyer, S. Park, C.W. Bielawski, R.S. Ruoff, *Chem. Soc. Rev.* **39** (2010) 228–240.
- A.C. Ferrari, J.C. Meyer, V. Scardaci, C. Casiraghi, M. Lazzeri, F. Mauri, S. Piscanec, D. Jiang, K.S. Novoselov, S. Roth, A.K. Geim, *PRL* **97** (2006) 187401.
- A. Dixit, G. Lawes, *J. Phys. Condens. Matter* **21** (2009) 456003.
- Z. An-Min, L. Kai, J. Jian-Ting, H. Chang-Zhen, T. Yong, J. Feng, Z. Qing-Ming, *Chin. Phys. B* **24** (2015) 126301.
- H. Zhang, X. J. Lv, Y. M. Li, Y. Wang and J. H. Li, *ACS Nano*, **4**, 380 (2010).
- Rauf, M. A.; Mehtani, M. A.; Khaleel, A.; Ahmed, A., *Chem. Eng. J.* 2010, **157**, 373–378.
- Li, H.; Zhu, M.; Chen, W.; Xu, L.; Wang, K., *J. Colloid Interface Sci.* 2017, **507**, 35–41.
- B. Wang, D. Guan, Z. Gao, J. Wang, Z. Li, W. Yang and L. Liu, *Materials Chemistry and Physics* **141**, 1 (2013).
- T. Lua, Y. Zhanga, H. Lia, L. Pana, Y. Lib, Z. Sun, *Electrochimica Acta* **55**, 4170 (2010).
- R. Wang, C. Xu, J. Sun, L. Gao and H. Yao, *ACS Appl. Mater. Interfaces*, **6**, 3427 (2014).
- X. Gao, W. Luo, C. Zhong, D. Wexler, S. -L. Cho, H.-K. Liu, Z. Shi, G. Chen, K. Ozawa and J.- Z. Wang, *Sci. Rep.* **4**, 6095 (2014).
- Raghvan, N.; Thangavel, S.; Venugopal, G., *Mater. Sci.Semicond. Process.* 2015, **30**, 321–329.
- H. Zhang, K. Ye, K. Zhu, R. Cang, J. Yan, K. Cheng, G. Wang, D. Cao, *Electrochim.Acta* **256** (2017) 357–364.

29. Y. Si, G. Liu, C. Deng, W. Liu, H. Li, L. Tang, J. Electroanal. Chem. 787 (2017) 19–23.

30. Z. Fang, F. Fan, Z. Ding, C. Wang, L. Long, S. Hao, Mater. Res. Bull. 48 (2013) 1737–1740.

4. **Has the progress been accordingly to original plan of work and towards achieving objectives if not, state reasons**
- Besides the project, some new objectives have been identified due to the potential of these materials in various applications i.e. photocatalytic and electrochemical applications.
- The additional plans were implemented due to the delay in the purchase process. It is also observed that having a project fellow would have improved the strategies in the implementation of the project.
5. **Please indicate the difficulties, if any, experienced in implementing the project**
- Due to the non – availability of man power the implementation of the project has been quite difficult.
- Also the purchase of equipment is significantly hampered due to non – availability of bidders (registered for the supply of the items, as per GFR 2005 (LTI))
6. **Details of Publications resulting from the project work (please attach re-prints) letter of Acceptance of paper communicated.**
1. A. Mishra et.al. *Rapid photodegradation of methylene blue dye by rGO- V2O5 nano composite*, *J. Alloys and Compounds* (doi.org/10.1016/j.jallcom.2020.155746) (In Press) (I.F. 4.15)
  2. A.Mishra, et.al. *Comparative electrochemical analysis of rGO-FeVO4 nanocomposite and FeVO4 for supercapacitor applications*, *App. Surf. Sci.* 488, 221(2019) (I.F.5.175)
  3. G. Bera, et.al. *Multifunctionality of Partially Reduced Graphene Oxide –CrVO<sub>4</sub> Nano-Composite: Electrochemical and Photocatalytic Studies with Theoretical Insight from Density Functional Theory*, *J. Phy. Chem C.* 122,21140 (2018) (I.F.4.37)
  4. Ganesh Bera, et.al. *Triclinic – monoclinic – orthorhombic (T–M–O) structural transitions in phasediagram of FeVO<sub>4</sub> -CrVO<sub>4</sub> solid solutions*. *Journal of Applied Physics* 122, 115101 (2017) (I.F. 2.10)
  5. Priyanath Mal, et.al. *Electronic, magnetic and spectroscopic properties of doped Mn(1-x)AxWO4(A = Co, Cu, Ni and Fe) multiferroic: an experimental and DFT study*. *Journal of Physics Condensed Matter*, 29, 075901(2017) (I.F.2.657)
  6. P.Rambabu et.al. *rGO- SnO<sub>2</sub> Composites for Super capacitor Applications*, *IOP Conf. Series: Materials Science and Engineering* 149 (2016) 012169
  7. P.Rambabu et.al. *Study of photocatalytic degradation of an industrial dye Ujala Supreme and Methyl Orange using SnO<sub>2</sub> – rGO composites* *AIP Conf. Proceedings* 1728 (2016) 020375
7. **Any other information which would help in evaluation of work done on the project**
- P.I. is also involved in other functional properties studies on orthovanadate compounds, which yielded interesting results and publications in *Phy Rev B*, *Scientific Reports*, *PCCP* etc. **One Student also submitted thesis in the field of Multiferroics who actively participated in the activities of UGC MRP partially**